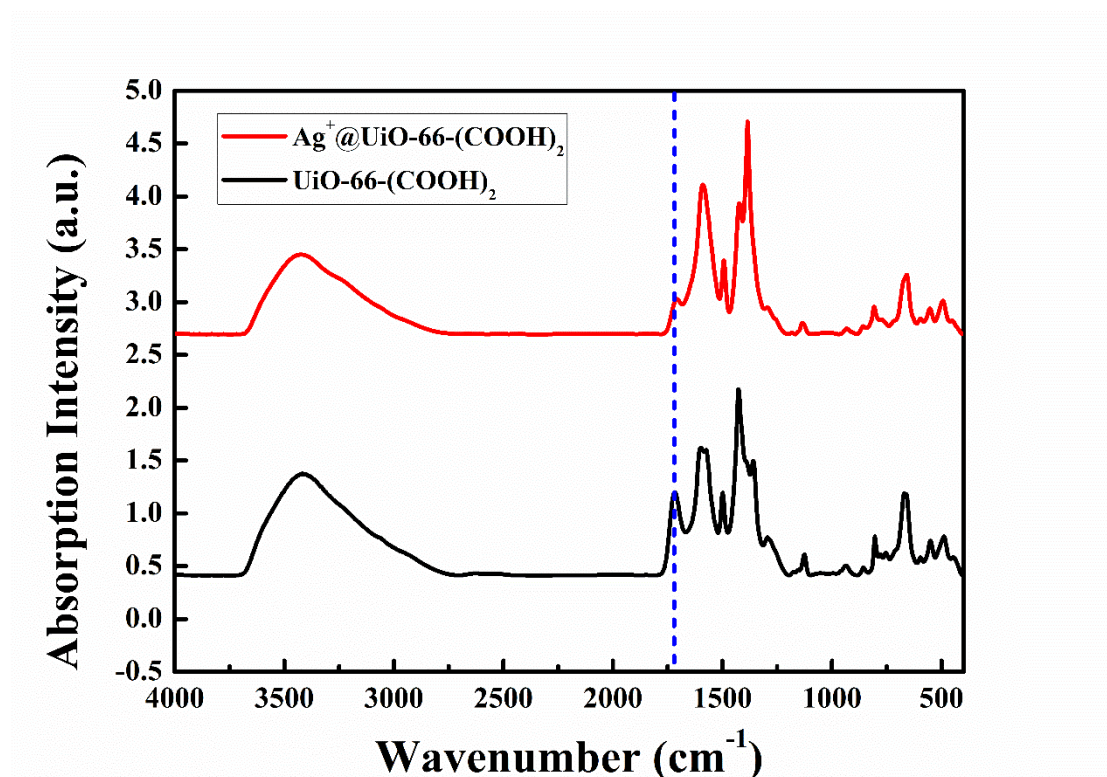
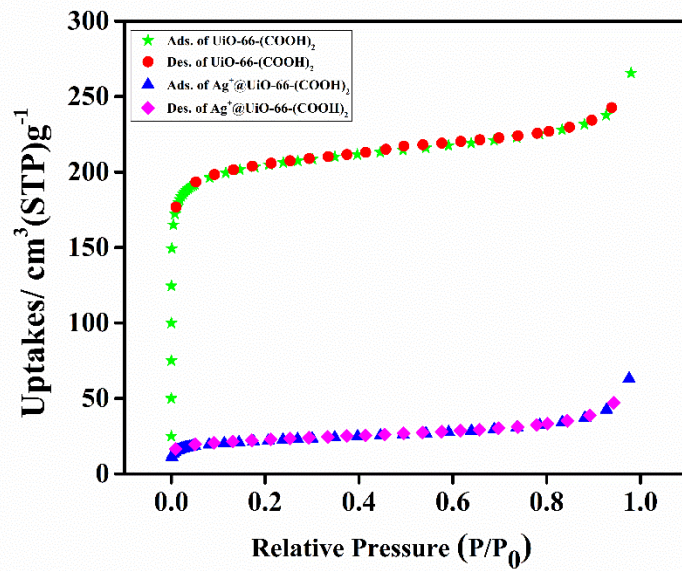


# Highly Sensitive Adsorption and Detection of Iodide in Aqueous Solution by a Post-Synthesized Zirconium-Organic Framework

Jun Zhang <sup>\*†</sup>, Shanli Yang <sup>†</sup>, Lang Shao, Yiming Ren, Jiaolai Jiang, Huaisheng Wang, Hao Tang, Hui Deng and Tifeng Xia <sup>\*</sup>



**Figure S1.** FT-IR spectra of  $\text{UiO-66-(COOH)}_2$  and  $\text{Ag}^+@\text{UiO-66-(COOH)}_2$ .



**Figure S2.** N<sub>2</sub> adsorption-desorption isotherms of UiO-66-(COOH)<sub>2</sub> and Ag<sup>+</sup>@UiO-66-(COOH)<sub>2</sub> at 77 K.

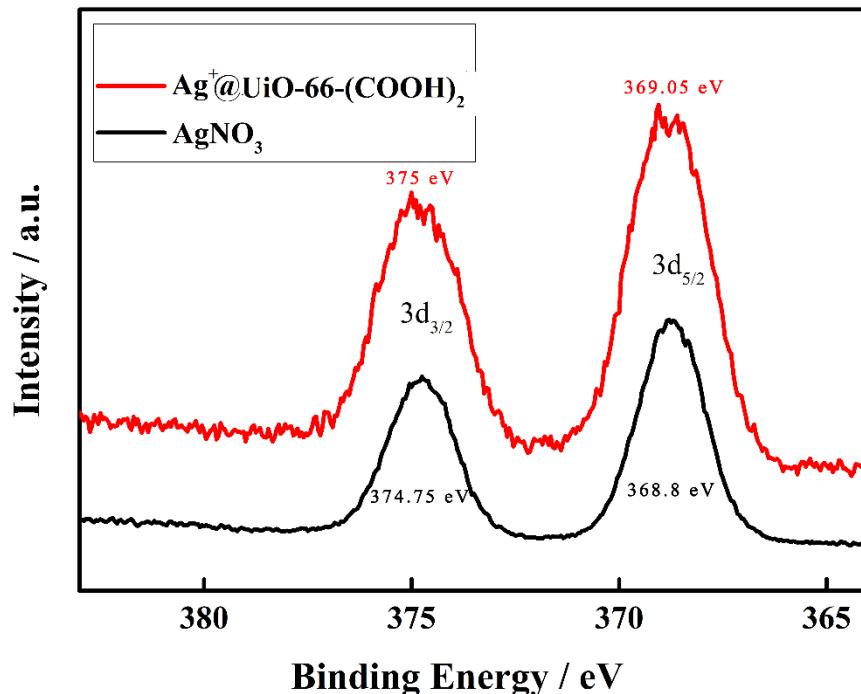


**Figure S3.** Survey XPS spectra of Ag<sup>+</sup>@UiO-66-(COOH)<sub>2</sub> and AgNO<sub>3</sub>.

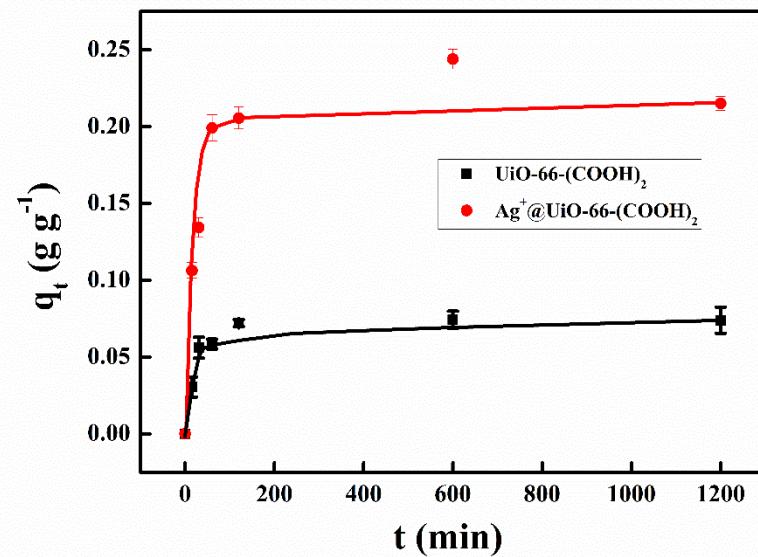


**Figure S4.** The effect of contact time on the I<sup>-</sup> adsorption on UiO-66-(COOH)<sub>2</sub> and Ag<sup>+</sup>@UiO-66-(COOH)<sub>2</sub> at room temperature.

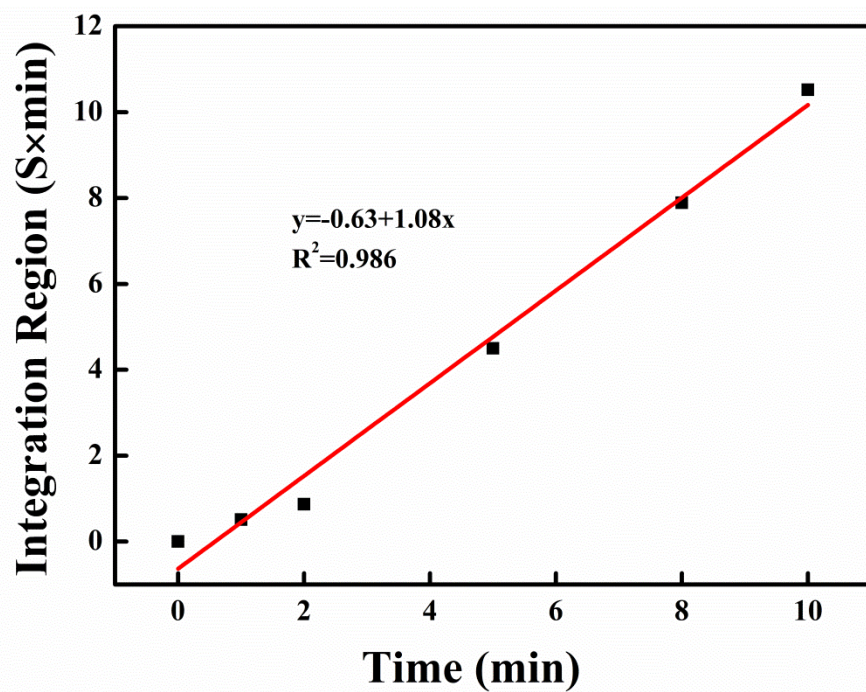


**Figure S5.** Standard curve of iodide in aqueous solution by ion chromatography.

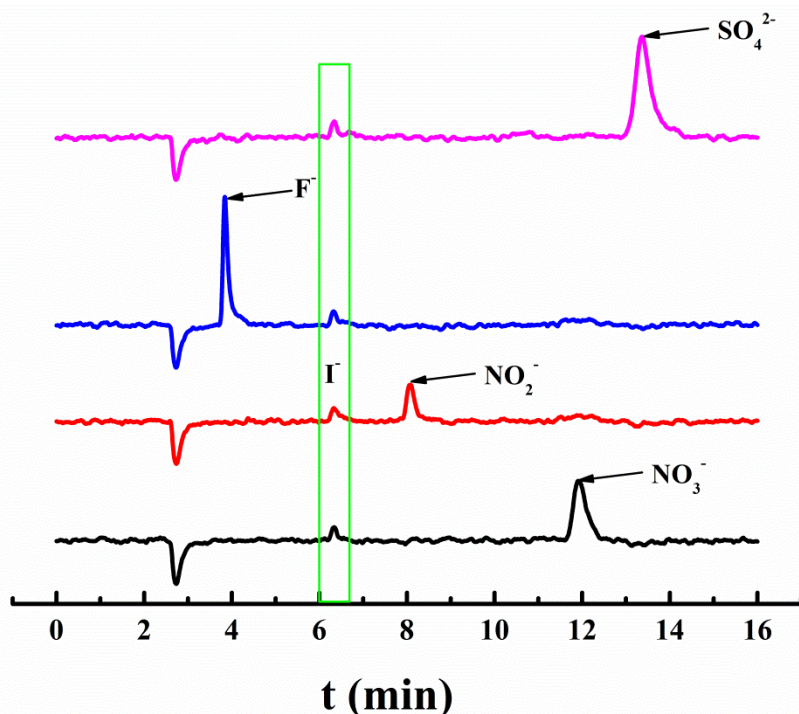


**Figure S6.** Ion chromatography of binary mixture containing I<sup>-</sup> and other competing anions.

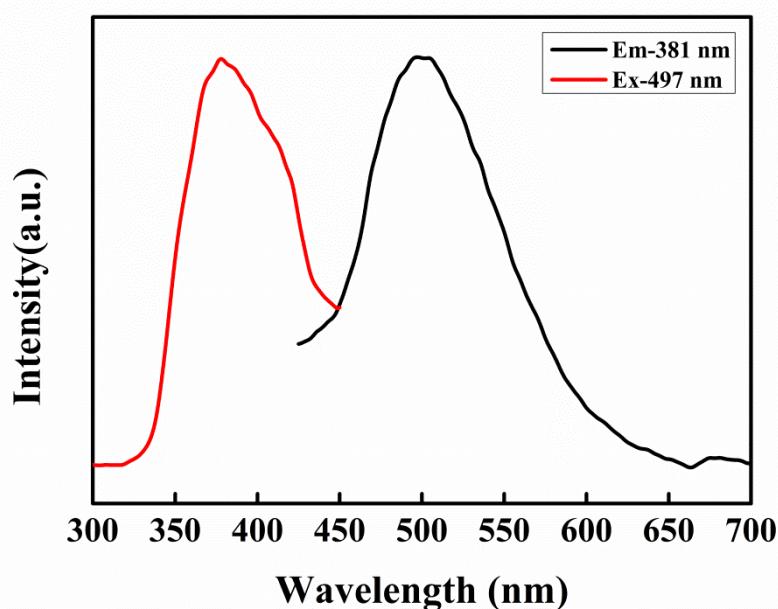


**Figure S7.** Excitation and emission spectra of Ag<sup>+</sup>@UiO-66-(COOH)<sub>2</sub> in aqueous solution.

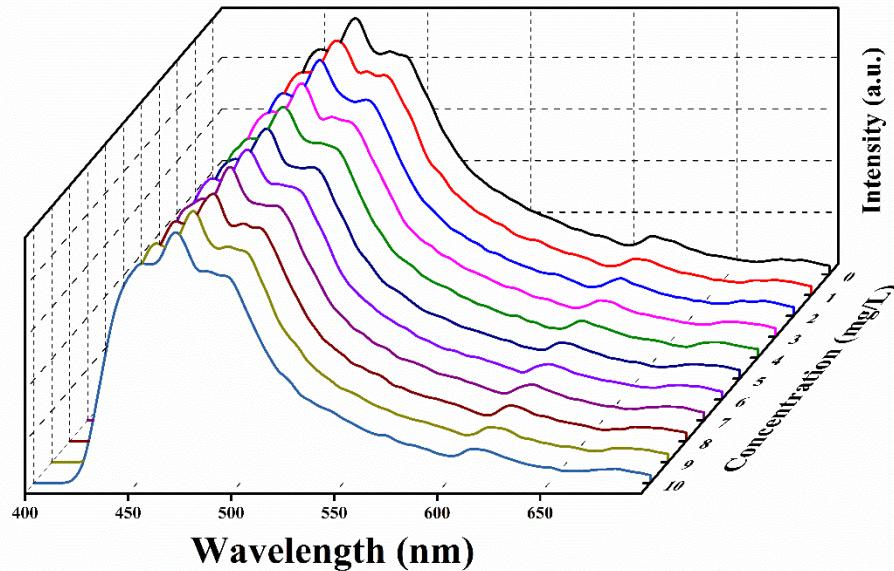


**Figure S8.** Emission spectra of  $\text{UiO-66-(COOH)}_2$  upon the addition of different concentration of  $\text{I}^-$ .

**Table S1.** Kinetics parameters for  $\text{I}^-$  adsorption on  $\text{Ag}^+@\text{UiO-66-(COOH)}_2$ .

Concentration	$k_2$	$Q_e$	$R^2$
500 mg/L	0.898 (g/(g·min))	221.2 mg/g	0.995

**Table S2.** The Langmuir isotherm model parameters for  $\text{I}^-$  adsorption on  $\text{Ag}^+@\text{UiO-66-(COOH)}_2$ .

Materials	$K_L$	$q_m$	$R^2$
$\text{UiO-66-(COOH)}_2@\text{Ag}^+$	11.81 (L/g)	235.5 mg/g	0.970

**Table S3.** Comparison of the iodide adsorption in different adsorbents.

Adsorbent	Adsorption capacity (mg/g)	Equilibrium time	Ref.
MIL-101(Cr)-SO <sub>3</sub> Ag	244.2	24 h	[1]
Nano Cu <sub>2</sub> O/Cu-C	41.2	10 min	[2]
25%-Ag@MIL-101	2.14	2 h	[3]
Mg/Al/Bi MMO	202.2	12 h	[4]
1.0%-Ag@Cu <sub>2</sub> O	25.38	2 h	[5]
Al <sub>2</sub> O <sub>3</sub> carbon fiber	46.15	2 h	[6]
MIL-101(Cr)@Ag	57	10 min	[7]
$\text{Ag}^+@\text{UiO-66-(COOH)}_2$	<b>235.5</b>	<b>20 h</b>	<b>This work</b>

**Table S4.** Comparison of the iodide sensing on different fluorescent probes.

Probes	Linear range	LOD	Ref.
<b>Gold nanoclusters</b>	1-100 $\mu\text{M}$	0.056 ppm	[8]
<b>Thymine</b>	0.01-1000 $\mu\text{M}$	0.64 ppb	[9]
<b>Cz-TPM</b>	100-800 $\mu\text{M}$	1.10 ppm	[10]
<b>OTf</b>	0-50 $\mu\text{M}$	0.025 ppm	[11]
<b>Cd-MOF</b>	0-25 $\mu\text{M}$	0.088 ppm	[12]
<b>IPF</b>	1-10 $\mu\text{M}$	0.11 ppm	[13]
<b>Ag<sup>+</sup>@UiO-66-(COOH)<sub>2</sub></b>	0.72-7.2 $\mu\text{M}$	0.58 ppm	This work

## References

- Zhao X.; Han X.; Li Z.; Huang, H.; Liu, D.; Zhong, C. Enhanced removal of iodide from water induced by a metal-incorporated porous metal-organic framework. *Appl. Surf. Sci.* **2015**, *351*, 760–764.
- Zhang X, Gu P, Li X, Zhang G, Efcient adsorption of radioactive iodide ion from simulated wastewater by nano Cu<sub>2</sub>O/Cu modified activated carbon. *Chem. Eng. J.* **2017**, *322*, 129–139.
- Mao P, Qi B, Liu Y, Zhao L, Jiao Y, Zhang Y, Jiang Z, Li Q, Wang J, Chen S, Yang Y, Ag-II doped MIL-101 and its adsorption of iodine with high speed in solution. *J. Solid State Chem.* **2016**, *237*, 274–283.
- Lee S-H, Takahashi Y, Selective immobilization of iodide onto a novel bismuth-impregnated layered mixed metal oxide: Batch and EXAFS studies. *J. Hazard. Mater.* **2020**, *384*, 121223.
- Mao P, Liu Y, Jiao Y, Chen S, Yang Y, Enhanced uptake of iodide on Ag@Cu<sub>2</sub>O nanoparticles. *Chemosphere*, **2016**, *164*, 396–403.
- Rong J, Zhao Z, Jing Z, Zhang T, Qiu F, Xu J, High-specific surface area hierarchical Al<sub>2</sub>O<sub>3</sub> carbon fiber based on a waste paper fiber template: preparation and adsorption for iodide ions. *J. Wood Chem. Technol.* **2017**, *37*, 485–492.
- Wan J, Li Y, Jiang Y, Yin Y, Silver-doped MIL-101(Cr) for rapid and effective capture of iodide in water environment: exploration on adsorption mechanism. *J. Radioanalytical Nuclear Chem.* **2021**, *328*, 1041–1054.
- Wang M, Wu Z, Yang J, Wang G, Wang H, Cai H, Au25(SG)18 as a fluorescent iodide sensor, *Nanoscale* **2012**, *4*: 4087–4090.
- Dai R, Wang X, Wang Z, Mu S, Liao J, Wen Y, Lv J, Huang K, Xiong X, A sensitive and label-free sensor for melamine and iodide by target-regulating the formation of G-quadruplex. *Microchem. J.* **2019**, *146*, 592–599.
- Dang Q, Wan H, Zhan X, Carbazolic porous framework with tetrahedral core for gas uptake and tandem detection of iodide and mercury, *ACS Appl. Mater. Interfaces* **2017**, *9*, 21438–21446.
- Salomón-Flores M, Hernández-Juárez C, Bazany-Rodríguez I, Barroso-Flores J, Martínez-Otero D, López-Arteaga R, Valdés-Martínez J, Dorazco-González A, Efficient fluorescent chemosensing of iodide based on a cationic meso-tetraarylporphyrin in pure water. *Sens. Actuators B* **2019**, *281*, 462–470.
- Singha D, Majee P, Mondal S, Mahata P, Luminescent cadmium based MOF as selective and sensitive iodide sensor in aqueous medium. *J. Photochem. Photobiol. A* **2018**, *356*, 389–396.
- Chen Z, Sun R, Feng S, Wang D, Liu H, Porosity-induced selective sensing of iodide in aqueous solution by a fluorescent imidazolium-based ionic porous framework, *ACS Appl. Mater. Interfaces* **2020**, *12*, 11104–11114.